Materials Science Forum
ISSN: 1662-9752, Vol. 1188, pp 45-55

Submitted: 2026-01-19
Revised: 2026-02-19
Accepted: 2026-02-22
Online: 2026-04-20

Effect of Interfacial Heat Transfer on the Solidification Behaviour of Numerically Simulated High-Pressure Die Casting Process

Nagasivamuni Balasubramani[1,a*] and Mohamed El Mansori[1,b]

[1]Materials, Surfaces, Mechanics and Processing Laboratoire, MSMP-EA7350, Arts et Métiers ParisTech, 2 cours des Arts et Métiers, 13617 Aix-en-Provence, France

[a]nagasivamuni.balasubramani@ensam.eu, [b]mohamed.elmansori@ensam.eu,

Keywords: Numerical simulation, high-pressure die casting, solidification, filling velocity

Abstract. The effect of time-dependent interfacial heat transfer coefficient (h) within the shot sleeve and die cavity of high pressure die casting process (HPDC) has been simulated to systematically study the solidification occurring during filling. Two different h-profiles have been considered with peak values of 7 kW/m^{2}K and 12 kW/m^{2}K for the shot sleeve, and 18 kW/m^{2}K and 24 kW/m^{2}K for the runner, gate, and die cavity based on the values reported in the literature. In addition, two types of gate designs were considered for plate type castings to analyze their solidification behaviour and filling velocity. For the A356 alloy investigated, solidification typically occurs along the bottom wall of the shot sleeve, from the mid-region toward the mould-side region along the direction of pouring. At the end of filling, the solid fraction (f_s) inside the shot sleeve increases from 10 to 18% with increasing peak value for h-profiles. Similarly, the progress of solidification around the gate regions increases rapidly above 0.4 f_s and reduces the channel width at the gate entry for h profile with higher peak values. Despite the lack of consensus on the selection of h value (peak value and range), this study highlights the influence h profiles and gating design on solidification during filling and discusses its implications on HPDC parts with large filling lengths.

Introduction

Aluminium alloy castings for automotive applications are predominantly produced via High pressure die casting (HPDC) process due to their versatility to produce complex shapes, thin sections, long flow lengths with better dimensional accuracy, production rate, and surface finish [1–3]. Despite these advantages, understanding the role of process variables in achieving product consistency and reducing defective parts remains highly challenging [1]. In a cold chamber HPDC, the important stages are filling the shot sleeve, high velocity injection of molten metal into the die cavity (2-4 m/s), and solidification under high pressure [3]. In general, defects formed in the HPDC process can be categorized into surface defects, subsurface defects, or internal and geometrical defects [1]. Filling, gas-related defects (air entrapment and H_2 content), and oxides are the most common defects that significantly affect the as-cast tensile strength and elongation. Both morphology, growth, and size distribution of bubbles play an important role in determining the as-cast tensile properties of the HPDC alloys [4]. Higher elongation values in the as-cast condition > 9% are achievable in HPDC when the size of the largest pore is controlled below 0.2 mm [2].

The second most influencing factor for porosity or related defects in HPDC is the formation of externally solidified crystals (ESCs) in the shot sleeve prior to the injection stage [5]. Nucleation of large, dendritic α-Al grains occurring inside the shot sleeve at relatively slower cooling rate could entrain into the die cavity causing shrinkage porosities due to restricted feeding or sometimes associated with defects (oxides). Despite constant operating parameters, occurrence and morphology of macro porosities varied significantly between trials [6], and it has been highlighted that the increase in feeding time by 0.25 s or more could affect the liquid volume by ± 3.5%. These small variations arise from several uncertainty factors such as cold flakes in gate regions, spray variation, local metal/mould temperature and other inclusions. The temperature gradient during filling around the gate regions is crucial in feeding and the development of defects like flow lines, cold laps, gas, and shrinkage porosities. [3]. Higher injection pressure near the corners and edges prevents the extensive

formation of a chilled layer, resulting in a better flow [7]. Restricted filling due to significant solid formation around the gate or the presence of unfragmented, large dendrites could affect the last stage of feeding during the intensification stage leading to porosities. Although the role of intensification pressure on reducing porosity (26% for 0 MPa to < 0.67% at 61 MPa) has been well acknowledged, the degree of macrosegregation, porosity/cracks observed near the gate to grip region of the sample is noticeable when solid fraction exceeds 0.5-0.6% [4].

Numerical simulations using finite element methods (FE) have provided a better visualization of the complex mould filling process and facilitated defect prediction during HPDC solidification. Research works by Dou et al. [8,9] have shown the effect of shot profile, solidification inside the shot sleeve, and the evolution of solid fraction during fast and slow shot speeds using FE simulations. Although the simulations are incapable of predicting the entrainment effect of pre-solidified phases (ESCs), it is highlighted that predicting the solidification occurring along the casting, gate, and runner regions during fast-filling stages is crucial to avoid defects. One of the most important thermal boundary conditions that can affect the accuracy of solidification is the interfacial heat transfer coefficient (h) between the liquid metal and the mould [10]. Inverse methodology is the most commonly used method for determining h values using temperature measurements from inside the dies. [11]. During the HPDC process, h values are estimated during the filling of the shot sleeve, fast filling stage (in the runner and gate regions), and intensification stage during solidification [11]. For different levels of intensification pressure, fast-shot speed, mould, and pouring temperature investigated by Koru and Serce [12], peak values of h value range from 11.8 to 15.7 kW/m^{2}K. Increasing intensification pressure from 80 to 60 MPa and velocity from 1.5-2.5 m/s increases the h value by 150-200 W/m^{2}K. Similarly, increasing pouring temperature and vacuum level increases h value, while increasing mould temperature reduces h. However, Yu et al. [13] have shown that the peak values of h at the entry point near the gate vary from 15 kW/m^{2}K to as high as 64 kW/m^{2}K and 16 to 26 kW/m^{2}K near the overfill region. By correlating the measured ESC size from the gate region and various locations within the sample, Sharifi et al. [14] revealed that h values could be in the range of 13 to 14 kW/m^{2}K. Highest peak values for h have been reported by Dargusch et al. [10] which ranges between 80-140 kW/m^{2}k for the intensification pressures of 32 MPa, 67 MPa, and 90 MPa. Moreover, it has been highlighted that the heat transfer is predominantly influenced by gate velocity and die temperature rather than the intensification pressure [10]. This is due to the mechanical constraints imposed by the progressive solidification restricting the effect of applied pressure. Similar values have been reported for h during the initial stages of die filling that ranges from 10^4 to 10^5 W/m^{2}K [5]. Under non-shooting conditions, where the liquid metal is left idle for 15 s after pouring into the shot sleeve (resembles the pouring of gravity casting), peak values of h are estimated to be in the range of values 4-6 kW/m^{2}K near the pouring zone, 10-14 kW/m^{2}K in the middle zone, and 8-12 kW/m^{2}K closer to the runner, respectively [15]. All these research work shows that there is a lack of agreement on the range and peak values of h during the HPDC process, which is affected by alloy type and processing conditions. Using a time-dependent h profile in FE simulations with a peak value of 10 kW/m^{2}K, Dou et al. [8] showed that nearly 11% of solid could form within 5 s idle time in the shot sleeve prior to the fast-filling stage. Though the second stage filling is expected to fragment these solid phases, the experimentally determined ESCs fraction is higher than the simulated solid fraction. This discrepancy could be due to the lower h values used in the simulations to predict the solid fraction during filling.

Therefore, the aim of this work is to simulate the h effect by assigning a time-dependent h profile to the shot sleeve and die cavity independently. The peak values for h-profile have been selected based on the literature (highest and lowest values reported in Al-Si alloys), and simulated for solid fractions along the shot sleeve, neck regions of the gate and drop in in-gate velocities as a function of time. The implications of having higher solid fractions around the gate and the importance of selecting a suitable h profile is briefly discussed.

Simulation Parameters and Procedures

Fig 1(a) shows the symmetrical 3D model consisting of moulds, piston, shot sleeve, casting, and overfill. A lean type runner system adopted from [16] and two different gating configurations adopted from [4,16] have been used to investigate the effect of filling velocity and solidification near the gate regions (Fig. 1(b)). The thickness and width of the traditional and trapezoidal gates are shown in Fig. 1(c). The simulation of filling and solidification during the HPDC process is performed using the HPDC module within the ProCAST software. The meshed surfaces of the 3D model using ProCAST solver are shown in Fig. 1(d). According to the previous work by the authors, mesh convergence is achieved when the sizes are below 1.5 mm [11]. Therefore, gradual meshing is employed for casting and shot sleeve volume with finer sizes (1 mm), and the remaining volumes are assigned as either 5 or 10 mm.

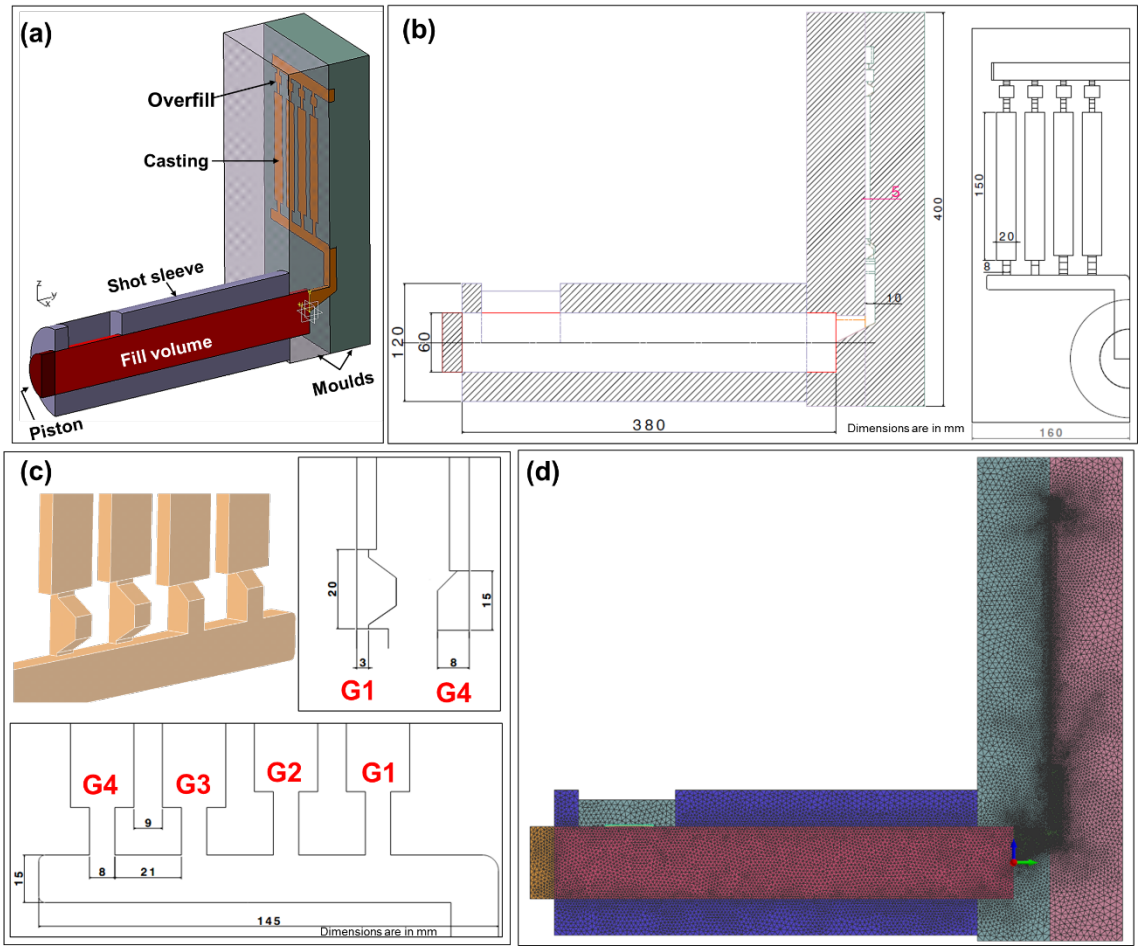

Fig. 1(a) 3D symmetrical model used for simulation, (b) 2D view highlighting the dimensions of the shot sleeve and mould. (c) Detailed view of the gate showing the dimensions and gate numbers. (d) Meshed 3D volume in ProCAST for all the volumes marked in (a).

Two different h-profiles were selected as shown in Fig. 2(a and b) based on Ref.[15] where h-profiles are experimentally determined for fill volumes ranging from 22% to 45%. For the first profile, h_{ss-1} (ss-shot sleeve) the curve shows one peak value at ~7 kW/m^{2}K and for h_{ss-2}, two peaks were imposed at the initial and final stages of filling as shown in Fig. 2(a). The filling and solidification within the shot sleeve are analysed without the piston displacement. Filling of the shot sleeve is performed at a very low filling velocity of 0.05 m/s to avoid significant turbulence. For the runner, gate, and mould regions two profiles (h_{rgm-1} and h_{rgm-2}) were selected as shown in Fig. 2(b). A higher peak value is imposed within 0.5 s, since the whole filling completes within a second. The cavity filling simulations were performed with the pre-existing melt volume (35% fill) inside the shot sleeve, and a shot delay time of 1s was applied for piston profile.

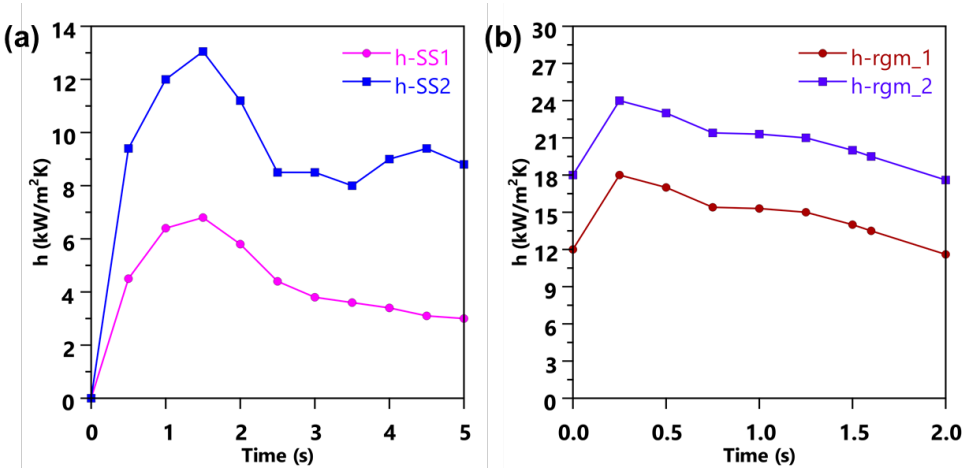

Fig. 2 Interface heat transfer ($\boldsymbol{h}$) profiles used in the simulation for (a) shot sleeve and (b) runner, gate and mould cavity regions.

The simulation parameters and thermodynamic properties of the Al-7Si alloy are listed in Table 1. The energy, mass, and momentum equations for an incompressible fluid flow are given as

$$\nabla \cdot v = 0 \text{ (Mass conservation)} \tag{1}$$

$$\rho\left(\frac{\partial v}{\partial t} + (v \cdot \nabla)v\right) = \nabla \cdot \mu(\nabla v + (\nabla v)^T) - \nabla P + \rho g \tag{2}$$

$$\rho c_e\left(\frac{\partial T}{\partial t} + v \cdot \nabla \mathrm{T}\right) = \nabla \cdot (k \nabla T) \tag{3}$$

where v is the velocity vector, ρ is the density, μ is the dynamic viscosity of the liquid melt, P is pressure, T is temperature, g is the acceleration due to gravity, c_e is the effective specific heat and k is the thermal conductivity. Additional details regarding the simulation parameters and the prediction of the heat transfer and solidification after pouring the liquid metal into the shot sleeve are detailed in the previous work of the authors [11]. The volume of fluid method is used to enable free surface fluid tracking and temperature dependent viscosity (Newtonian flow), density and enthalpy models are used for the filling simulation.

Table 1 List of fixed and variable processing parameters used in the simulation [11]

Variables/ conditions	Value/range/specifications
Alloy composition (wt.%)	Al-7Si-0.3Mg (A356/EN AC-42100)
Onset temperature of α -Al (°C)	615.5
Solidus temperature (°C)	554.5
Dendritic coherency temperature, 0.30% f_s^{coh} (°C)	593-597
Pouring temperature, T_p (°C)	700
Shot sleeve, piston and mould temperature, T_{ss} (°C)	200
Fill volume of metal inside shot sleeve, f_v (%)	35
Interface heat transfer coefficient between alloy volume and shot sleeve, h (kW/m^{2}K)	h_{ss-1} and h_{ss-2}
Interface heat transfer coefficient between casting volume and runner/gate/mould, h (kW/m^{2}K)	h_{rgm-1} and h_{rgm-2}
Interface heat transfer coefficient between mould walls h (kW/m^{2}K)	2
Piston displacement velocity (m/s)	0.3/3.0 (slow/fast shot speeds)

To analyse the effect of h on the solidification, it is assumed that the defect formation is closely related to the shearing of partially solidified dendrites, coherency, and packing fraction of the solid proposed by Santos et al. [17]. Solid fractions below the dendritic coherency temperature (f_s^{coh}) is

assumed to behave similar to liquid and mass feeding is dominant (~0.30 for A356 alloy). After f_s^{coh} until packing point where the resistance to flow is minimal, flow can occur in liquid films (also called shear bands) in these regions by either mass or interdendritic feeding. Above this packing range (~0.4-0.5), the application of force encounters a solid network which might lead to cracks or voids that are unfilled, where liquid segregations may occur.

Results

Effect of h_{ss-1} and h_{ss-2} on the solidification behaviour within the shot sleeve

Fig. 3(a and b) shows the snapshots of solid fraction during filling for (a) h_{ss-1} and (b) h_{ss-2} profiles. At 1.5 s in Fig. 3(a and b), solidification occurs in the middle region of the shot sleeve, obstructing the flow initially due to the imposed peak value of h for both curves (Fig. 2(a)). The total percentage of solids increases rapidly from 0 to 10%, which is reduced to 9.3% by remelting due to the continuous flow of hot liquid from the pouring zone at 3.0 s (Fig. 3(a)). However, after 5s the solidified layers continue to develop along the bottom walls of the shot sleeve from the center region to the mould side along the longitudinal direction. Complete filling is achieved at 6s with nearly 14% solid fraction.

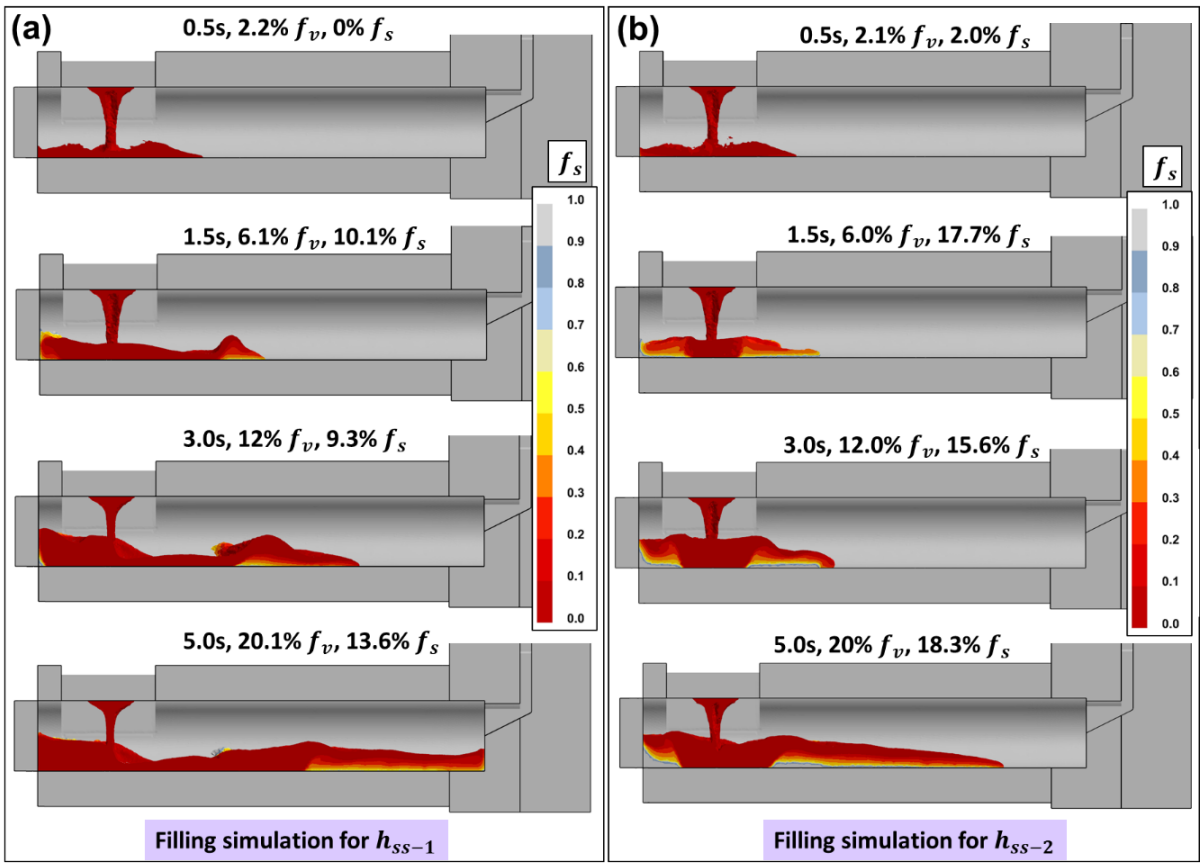

Fig. 3 Sectional view of the shot sleeve showing solidification along the wall regions during filling for (a) h_{ss-1} and (b) h_{ss-2} profiles

Solidification in Fig. 2(b) occurs at a relatively faster rate immediately after pouring due to a higher peak value used in h_{ss-2} as shown from 1.5 to 3.0 s. The solid fraction continues to increase and pose a significant resistance to the liquid flow. Complete filling in Fig. 3(b) is achieved at 7.5 s with nearly a 5% increase in the solid fraction compared to Fig. 3(a). The solidified layer near the pouring zone in Fig. 3(b) between 3 and 5s undergoes insignificant remelting due to the imposed second peak in the h_{ss-2} profile (Fig. 2(a)).

Fig. 4(a) shows the locations of point analysis along the bottom walls of the shot sleeve. Based on the previous work of the authors [11], it has been found that the solidification is more rapid near the

walls, between 1 to 5 mm after employing a constant value for h from 5000 to 20,000 W/m^{2}K. Since the largest dendrites with sizes ranging over 0.5-1 mm solidify in these slow cooled regions, cooling curves are presented at 2 mm and 5 mm respectively in Fig. 4(b-e). For h_{ss-1} profile, the cooling curves in Fig. 4(b) shows higher initial temperature above liquidus in the middle zone and solidifies slower compared to Fig. 4(c) in the locations closer to the mould side. For h_{ss-2}, a significant drop in the initial temperature below liquidus is noted in Fig. 4(d and e), indicating the formation of a higher volume fraction of ESCs during and after complete filling. In addition, a higher cooling rate and the time to reach solidus temperature is significantly reduced for h_{ss-2} in Fig. 4(e).

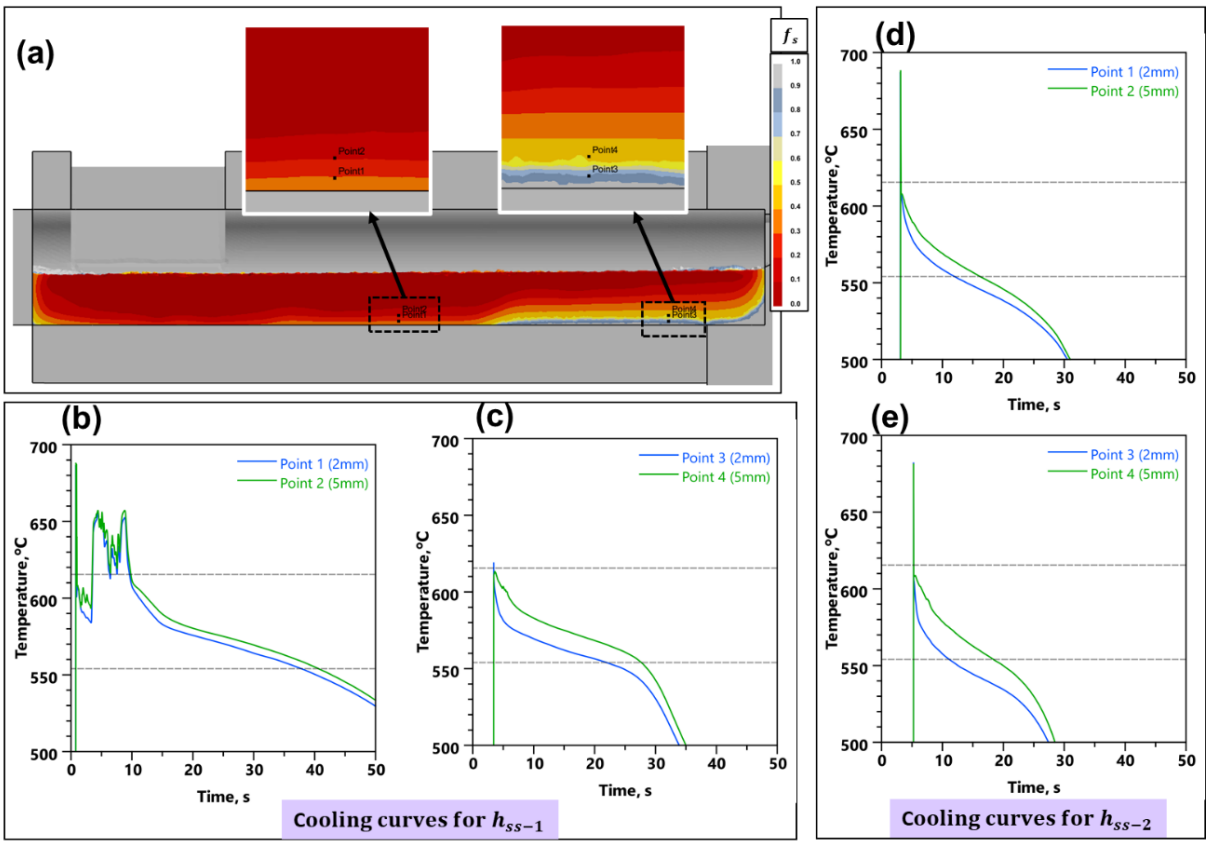

Fig. 4 (a) Sectional view of shot sleeve indicating the points at 2 mm and 5 mm from the bottom of the shot sleeve located at 190 mm (P1, P2) and 330 mm (P3, P4). Cooling curves at P1-P4 plotted for (b, c) $\boldsymbol{h_{ss-1}}$ and (d, e) $\boldsymbol{h_{ss-2}}$ profiles.

Effect of h_{grm-1} and h_{grm-2} on the solidification behaviour inside runner and gate regions

One of the main limitations with the FE solver is that the solid formation within the shot sleeve is an indication of how much pre-solidification occurs before injecting the melt into the die cavity. Most of the solids formed within the shot sleeve stay in the chamber walls and only the remaining liquid is injected into the runner and die cavity [8,11]. Therefore, the effect of pre-solidification affecting further flow and filling of runner or gate regions could not be predicted effectively [8]. Nevertheless, the effect of imposed h-profiles could still be useful to understand the effect of solidification occurring on the runner and gate regions, and it can be assumed that any presence of unfragmented, long dendrites would increase the severity of filling defects. Because a smoothed particle hydrodynamics simulation has revealed that solid fraction up to 0.8 could be fragmented from the bottom regions of the walls during filling and can settle in the runner or block the liquid movement in the gate regions [18].

Fig. 5 shows the snapshots of filling velocity, temperature and solid fraction for h_{grm-1} profile. To reduce the computational time, the mesh sizes for the fill volume in the shot sleeve and mould have been increased to 5 mm and 10 mm respectively, and 1 mm is applied to the runner, gate, and

casting volume. As shown in Fig. 5 (a), the filling starts initially at gates G3 and G4 and then proceeds to G1 and G2. The temperature and solid fraction curves indicate that there is no significant solid formation (Fig. 5 (b, c) at this stage. Notably, the velocity at the onset of G1 and G2 in Fig. 5 (d) is relatively higher compared to G3 and G4. This is because the trapezoidal gate design contains additional narrower cross sections closer to the runner as shown in Fig. 1(c). The corresponding temperature and solid fraction snapshots indicate that there is no significant drop or solidification during filling (< 0.3 f_s). The total filling time is around 1.6 s and the total solid percentage at complete filling is 31.1%.

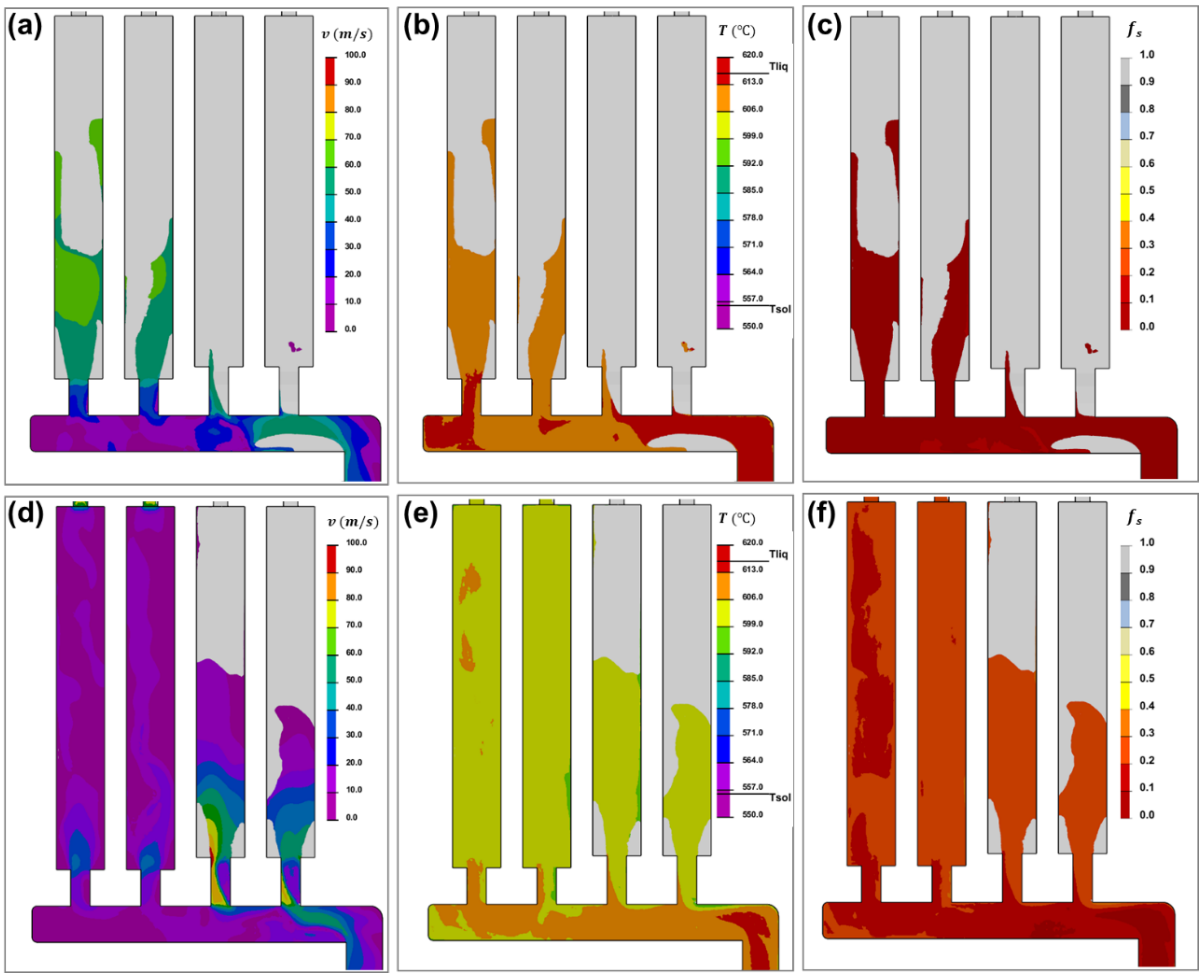

Fig. 5 (a, d) Fluid velocity, (b, c) temperature and (e, f) solid fraction at the onset of filling at the gates (a-c) G3, G4 and (d-f) G1, G2, respectively for $\boldsymbol{h_{grm-1}}$ profile.

To further understand the effect of fluid velocity and the development of solid fraction at the gate entry, point analysis from the middle region of each gate are plotted for h_{grm-1} and h_{grm-2} as shown in Fig. 6(a). Note that the snapshots shown in Fig. 5 are more representative of the solidification than point analysis, however, point analysis helps to correlate the fluid velocity and solid fraction as a function of time. In Fig. 6(b and c), the velocity profile in G3 and G4 increases progressively, while the increase in G1 and G2 is rapid at the onset of filling. In addition, G1 and G2 shows a two-stage curve where higher velocities are noted until 0.1-0.2f_s and drops to less than 40 m/s after 0.2f_s . Higher velocities during the initial stage of filling could break larger ESCs compared to a more gradual increase in filling velocity. In general, the solidification occurs relatively faster for h_{grm-2}, a higher f_s is noticed during the velocity cutoff. It should be noted that these f_s are formed during filling and did not account any ESCs. Any presence of large ESCs could reduce the filling velocity further.

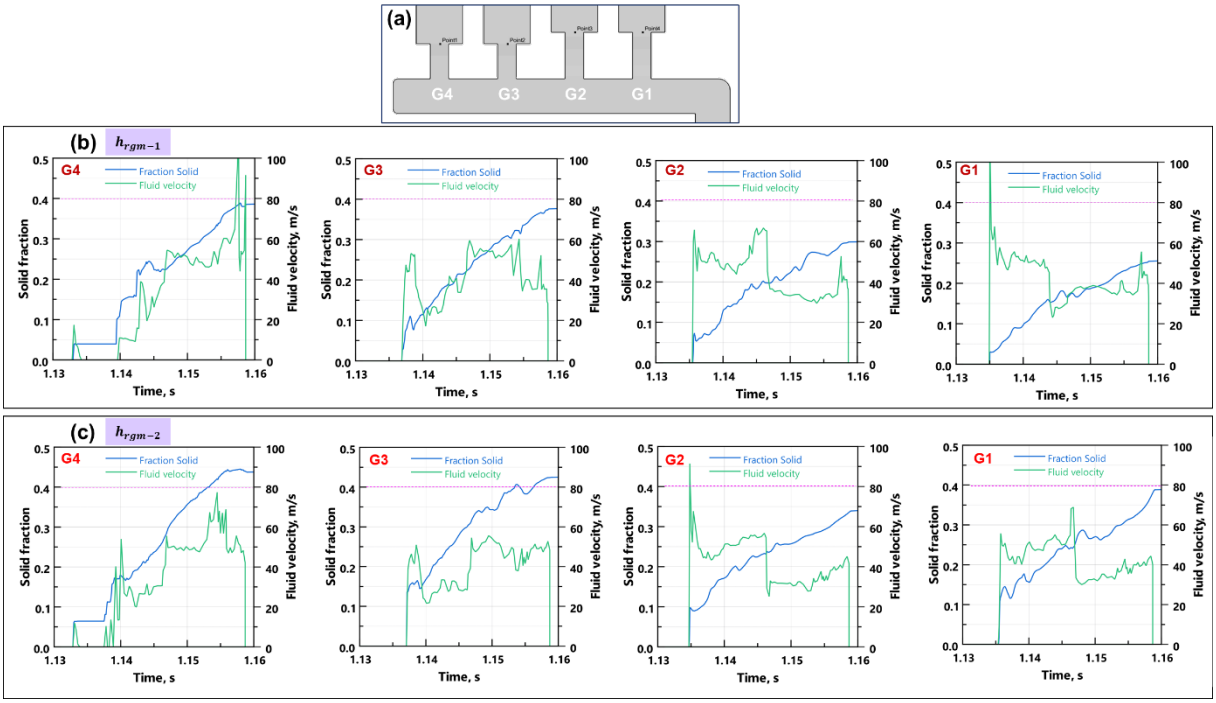

Fig. 6 (a) Cropped view of gate region of the casting highlighting the points located at gate entry analysed for filling velocity profile and solid fraction for profiles (b) $\boldsymbol{h_{grm-1}}$ *and (c)* $\boldsymbol{h_{grm-2}}$.

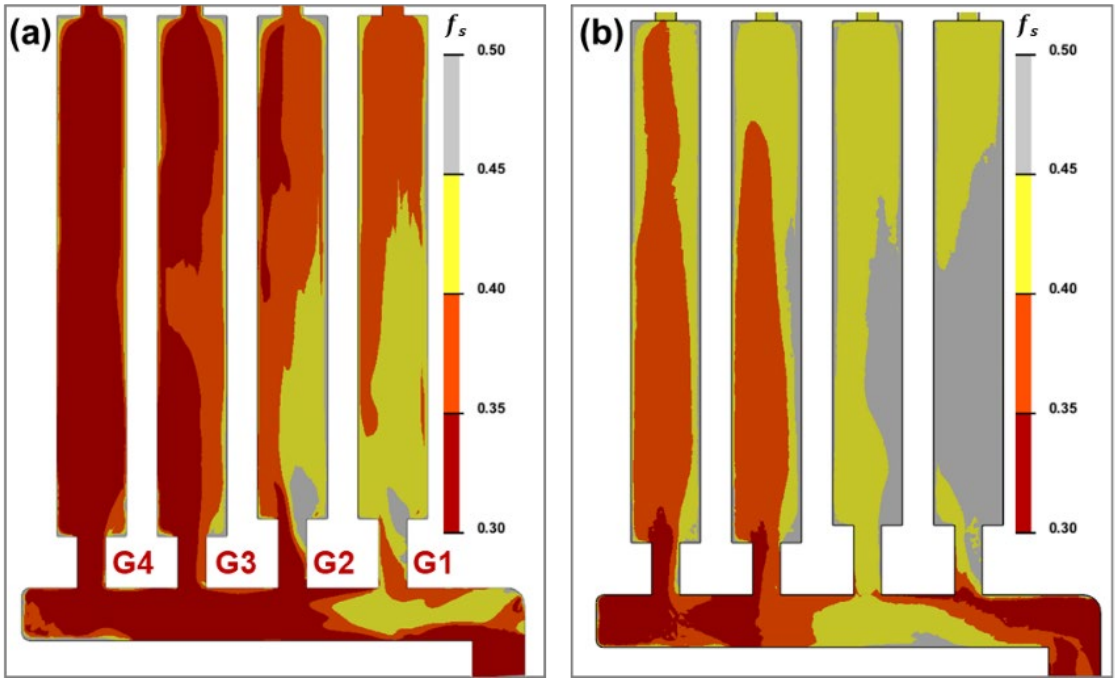

Fig. 7 Solid fraction snapshot at 1.15s highlighting the progress in solidification at the gate region for (a) $\boldsymbol{h_{grm-1}}$ and (b) $\boldsymbol{h_{grm-2}}$ profiles.

Fig. 7(a and b) shows the solid fraction snapshot at 1.15 s for h_{grm-1} and h_{grm-2} profiles, respectively. For G4 and G3, the solidification proceeds relatively slower compared to G1 and G2, due to the design of mould with thicker sections closer to G1. For the profile h_{grm-2}, the solidification occurring near the gate region reaches at 0.4-0.5 f_s during the last stages of filling (97%). Further increase in f_s above this range or the presence of ESCs in this region poses a risk for reducing the filling velocity and feeding related defects during the intensification stage.

Discussion

Prediction of solidification within the shot sleeve is significantly influenced by the h profile. Since most of the solid formation occurs along the length of the sleeve, a higher percentage of solidification indicates more entrainment of ESCs into the die cavity. Therefore, a higher filling velocity at the gate during filling is critical to reduce the blocking effect of ESCs and feeding restriction during intensification stages [18]. Gunasegaram et al. [19] demonstrated that the pore volume fraction decreases when gate velocities are raised from 26 to 82 m/s, and high integrity castings are obtained at 82 m/s gate velocity. Although increasing gate velocity offers porosity reduction, finer dendritic sizes, and efficient feeding, higher gate velocities are not recommended due to mould erosion risk. Microstructure showed more refined grains at gate velocity of 82 m/s similar to the rheocasting process, while at 25 m/s the large unbroken dendrites (ESCs) could be seen. Similar observations have been reported by Niu et al. [20] where increasing intensification pressure along with gate velocity from 33 m/s to 61 m/s decreases the presence of larger ESCs near the gate. It has been reported that for Al-Si-Cu alloys solidification strength develops between 0.3 f_s and 0.6 f_s [21]. Higher shearing rates induced by HPDC filling is expected to enable the filling by lowering the apparent viscosity for the solid fraction as high as 0.6 f_s [22]. However, the effect of continuous cooling due to higher values of h and drop in velocity/pressure and gate dimensions could affect this observation and has not been reported systematically in simulation studies. An increase in the peak value of h from 18 to 24 kW/m^2 shows a relatively higher solid fraction in the gate regions (Fig. 6) and reducing the gate width between 0.4 to 0.5 f_s (Fig. 7). It should be noted that the higher fluid velocity and lower viscosity could enable filling in these conditions for small flat castings demonstrated in the present work. However, for larger flow lengths and thin section castings, a systematic study on h is crucial to avoid defects. Secondly, it should also be highlighted that the initial solidification within the shot sleeve is not considered in the die filling. Generally, it has been agreed that the formation of solid fractions above 10% within the shot sleeve prior to filling can cause additional restrictions to both filling and feeding; defect band formation during the application of intensification pressure. Since the effect of h is greatly influenced by the combination of other processing variables such as fill volume and fill length, alloy composition, and gating system design, literature comparison becomes difficult. Further systematic works are necessary to address the effect of h on different longer filling lengths of castings and shot sleeves.

Conclusions

Solidification within the shot sleeve and gate regions during filling was simulated for plate-type castings with two gate geometries and four interfacial heat transfer coefficient profiles (h). Within the shot sleeve, solidification predominantly occurs from the middle region to the mould side. The h-profile with a peak value of approximately 7 kW/m^{2}K results in ~ 13% f_s, which increases to ~18% f_s for 13 kW/m^{2}K after complete filling. In the gate regions, increasing the peak values for h-profiles from 18 kW/m^{2}K to 24 kW/m^{2}K promotes local solidification between 0.4-0.5 f_s, reducing the width of the channel and flow velocities. Compared to the conventional gate design, the trapezoidal gate exhibits a higher fluid velocity during filling until 0.4 f_s. For a given gate design, this study emphasizes that accurate prediction of f_s based on h-profiles during shot sleeve filling and injection stages is necessary to ensure high-integrity HPDC components.

References

[1] F. Bonollo, N. Gramegna, G. Timelli, High-Pressure Die-Casting: Contradictions and Challenges, JOM 67 (2015) 901–908. https://doi.org/10.1007/s11837-015-1333-8.

[2] Y. Zhang, E. Lordan, K. Dou, S. Wang, Z. Fan, Influence of porosity characteristics on the variability in mechanical properties of high pressure die casting (HPDC) AlSi7MgMn alloys, J. Manuf. Process. 56 (2020) 500–509. https://doi.org/10.1016/j.jmapro.2020.04.071.

[3] A.R. Adamane, L. Arnberg, E. Fiorese, G. Timelli, F. Bonollo, Influence of Injection Parameters on the Porosity and Tensile Properties of High-Pressure Die Cast Al-Si Alloys: A Review, Inter. Metalcast. 9 (2015) 43–53. https://doi.org/10.1007/BF03355601.

[4] S. Otarawanna, H.I. Laukli, C.M. Gourlay, A.K. Dahle, Feeding Mechanisms in High-Pressure Die Castings, Metall. Mater. Trans. A 41 (2010) 1836–1846. https://doi.org/10.1007/s11661-010-0222-6.

[5] S. Otarawanna, C.M. Gourlay, H.I. Laukli, A.K. Dahle, Microstructure Formation in AlSi4MgMn and AlMg5Si2Mn High-Pressure Die Castings, Metall. Mater. Trans. A 40 (2009) 1645–1659. https://doi.org/10.1007/s11661-009-9841-1.

[6] D. Blondheim, A. Monroe, Macro Porosity Formation: A Study in High Pressure Die Casting, Inter. Metalcast. 16 (2022) 330–341. https://doi.org/10.1007/s40962-021-00602-x.

[7] X.P. Niu, K.K. Tong, B.H. Hu, I. Pinwill, Cavity pressure sensor study of the gate freezing behaviour in aluminium high pressure die casting, Int. J. Cast Met. Res.11 (1998) 105–112. https://doi.org/10.1080/13640461.1998.11819264.

[8] K. Dou, Y. Zhang, E. Lordan, A. Jacot, Z. Fan, Understanding the Initial Solidification Behavior for Al–Si Alloy in Cold Chamber High-Pressure Die Casting (CC-HPDC) Process Combining Experimental and Modeling Approach, Metall. Mater. Trans. A 53 (2022) 3110–3124. https://doi.org/10.1007/s11661-022-06731-0.

[9] K. Dou, E. Lordan, Y.J. Zhang, A. Jacot, Z.Y. Fan, A complete computer aided engineering (CAE) modelling and optimization of high pressure die casting (HPDC) process, J. Manuf. Process. 60 (2020) 435–446. https://doi.org/10.1016/j.jmapro.2020.10.062.

[10] M.S. Dargusch, A. Hamasaiid, G. Dour, N. Balasubramani, D.H. StJohn, The Influence of In-Cavity Pressure on Heat Transfer and Porosity Formation During High-Pressure Die Casting of A380 Alloy, JOM 72 (2020) 3798–3805. https://doi.org/10.1007/s11837-020-04341-y.

[11] N. Balasubramani, A. Ktari, M. El Mansori, Numerical simulation of solidification within the shot sleeve of high-pressure die casting and the prediction of secondary dendrite arm spacing for externally solidified crystals, Materialia 42 (2025) 102479. https://doi.org/10.1016/j.mtla.2025.102479.

[12] M. Koru, O. Serçe, Experimental and Theoretical Investigation of Heat Transfer in Vacuum Assisted High Pressure Die Casting (HPDC) Process, Inter. Metalcast. 18 (2024) 3013–3027. https://doi.org/10.1007/s40962-023-01217-0.

[13] W. Yu, S. Liang, Y. Cao, X. Li, Z. Guo, S. Xiong, Interfacial heat transfer behavior at metal/die in finger-plated casting during high pressure die casting process, China Foundry 14 (2017) 258–264. https://doi.org/10.1007/s41230-017-6066-6.

[14] P. Sharifi, J. Jamali, K. Sadayappan, J.T. Wood, Grain Size Distribution and Interfacial Heat Transfer Coefficient during Solidification of Magnesium Alloys Using High Pressure Die Casting Process, J. Mater. Sci. Technol. 34 (2018) 324–334. https://doi.org/10.1016/j.jmst.2016.09.004.

[15] W. Yu, Y. Cao, Z. Guo, S. Xiong, Development and application of inverse heat transfer model between liquid metal and shot sleeve in high pressure die casting process under non-shooting condition, China Foundry 13 (2016) 269–275. https://doi.org/10.1007/s41230-016-5137-4.

[16] E. Lordan, K. Dou, Y. Zhang, C. Tzileroglou, A. Jacot, P. Blake, Z. Fan, Turbulent breakup of non-metallic inclusions and equiaxed crystals during solidification of a hypoeutectic Al-Si alloy, Materialia 17 (2021) 101114. https://doi.org/10.1016/j.mtla.2021.101114.

[17] J. Santos, A.E.W. Jarfors, A.K. Dahle, Filling, Feeding and Defect Formation of Thick-Walled AlSi7Mg0.3 Semi-Solid Castings, SSP 256 (2016) 222–227. https://doi.org/10.4028/www.scientific.net/SSP.256.222.

[18] H. Tokunaga, Y. Motoyama, T. Okane, Particle Method Simulation for Formation and Flow of Cold Flakes in High-Pressure Die Casting, Inter. Metalcast. 13 (2019) 897–904. https://doi.org/10.1007/s40962-019-00306-3.

[19] D.R. Gunasegaram, B.R. Finnin, F.B. Polivka, Melt flow velocity in high pressure die casting: Its effect on microstructure and mechanical properties in an Al–Si alloy, Mater. Sci. Technol. 23 (2007) 847–856. https://doi.org/10.1179/174328407X176992.

[20] X.P. Niu, K.K. Tong, B.H. Hu, I. Pinwill, Cavity pressure sensor study of the gate freezing behaviour in aluminium high pressure die casting, Int. J. Cast Met. Res. 11 (1998) 105–112. https://doi.org/10.1080/13640461.1998.11819264.

[21] A.K. Dahle, T. Sumitomo, S. Instone, Relationship between tensile and shear strengths of the mushy zone in solidifying aluminum alloys, Metall. Mater. Trans A 34 (2003) 105–113. https://doi.org/10.1007/s11661-003-0212-z.

[22] D.R. Gunasegaram, M. Givord, R.G. O'Donnell, B.R. Finnin, Improvements engineered in UTS and elongation of aluminum alloy high pressure die castings through the alteration of runner geometry and plunger velocity, Mater. Sci. Eng. A 559 (2013) 276–286. https://doi.org/10.1016/j.msea.2012.08.098.